Low-noise preamplifier with input and feedback transformers for low source resistance sensors

J. Lepaisant, M. Lam Chok Sing, and D. Bloyet
Laboratoire d'Electronique et d'Instrumentation, Institut des Sciences de la Matière et du Rayonnement, Boulevard du Maréchal Juin, F 14050, Caen Cedex, France

(Received 7 August 1991; accepted for publication 30 September 1991)

We describe the design, schematics, and performances of a very-low-noise, low-frequency preamplifier. It operates in the 5 Hz–100 kHz range and offers an input equivalent voltage noise density as low as 65 pV/$\sqrt{\text{Hz}}$; the current noise increases with frequency and settles to about 1.5 pA/$\sqrt{\text{Hz}}$ at 100 kHz. The amplifier uses input and feedback signal transformers and operates in full differential mode; a $-$ 163 dB common-mode rejection ratio is achieved at line frequency. Design methodology is applicable to other ranges of frequencies.

I. INTRODUCTION

Some low-level, low-impedance sensors, typically dc SQUIDs, have to be connected to low-noise, low-resistance preamplifiers in order to take profit of their high intrinsic resolution. Equivalent input noise voltage of a few 10 pV/$\sqrt{\text{Hz}}$ and optimal noise resistance of a few ohms are typical values which have to be achieved. In order to reach such a level of performance, two techniques are currently used. In the first one, the sensor is associated to a coil to form a high-quality factor LC tank circuit; it is therefore frequency selective. On the contrary, the other one offers a much wider frequency range since it makes use of an up-signal transformer.

We have designed an input and feedback transformer preamplifier whose input noise voltage is as low as 65 pV/$\sqrt{\text{Hz}}$ and whose frequency range extends at a low source impedance from 5 Hz to about 100 kHz. In Sec. II we discuss within some calculation of the amplifier optimization in terms of noise, bandwidth, and long-term gain stability. The second part gives a closer analysis of the designed structure while the last part presents experimental results on both the signal and noise points of view.

II. THE INPUT TRANSFORMER COUPLED FEEDBACK PREAMPLIFIER: PRINCIPLE AND PERFORMANCES

Preamplifier noise performances come mainly from their first stage contribution; by an appropriate choice of active devices and bias conditions, optimal source resistance of a few 10 Ω can be obtained.[1,2] However, for sensors of much lower source resistances, input transformer coupling must be introduced if a wide frequency response is to be obtained.[3,4] Characteristics of such an arrangement can be greatly enhanced in terms of gain stability and low cutoff frequency by the introduction of parallel-serial feedback, as shown schematically in Fig. 1(a). Figure 1(b) gives a more detailed description of this circuit and allows calculations of both the input–output transfer function and noise characteristics.

Let us first express the amplifier output voltage v_0 as a function of the three independent generators e_S, e_A, and i_A; it becomes

$$v_0 = \frac{jAM_F\omega/Z_1}{1+jH_0(AM_F\omega/Z_1)} \times\left(e_S + e_A\frac{Z_1}{jM_F\omega} - \frac{\omega^2M_F^2 + Z_1Z_2}{jM_F\omega}\, i_A\right), \tag{1}$$

where

$$Z_1 = R_S + R_{F_1} + R_0 + jL_{F_1}\omega,$$

$$Z_2 = R_{F_2} + jL_{F_2}\omega,$$

and

$$M_F = \sqrt{L_{F_1}L_{F_2}} = N_F L_{F_1}.$$

In expression (1), R_{F_1} (respectively R_{F_2}) and L_{F_1} (respectively L_{F_2}) are the resistance and self-inductance of the transformer windings with a coupling factor assumed to be unity and a transformation ratio noted as N_F; R_S stands for the source resistance and A is the amplifier gain.

A. Signal analysis

From expression (1) and for $e_A = i_A = 0$, it is clear that the amplifier transfer function is of a first-order high-pass type. As expected, at high frequency and high loop gain, the v_0/e_S ratio is only dependent on H_0 while the low cutoff frequency, which is expressed as

$$f_0 = \frac{R_S + R_0 + R_{F_1}}{2\pi L_{F_1}(1 + AH_0N_F)}, \tag{2}$$

is, compared to its open-loop value, lowered by the loop gain factor.

B. Noise analysis

From expression (1), the preamplifier equivalent input noise density noted $e_{n_T}^2$ can also be obtained in an easy way.[5] It becomes

 0034-6748/92/032089-06$02.00

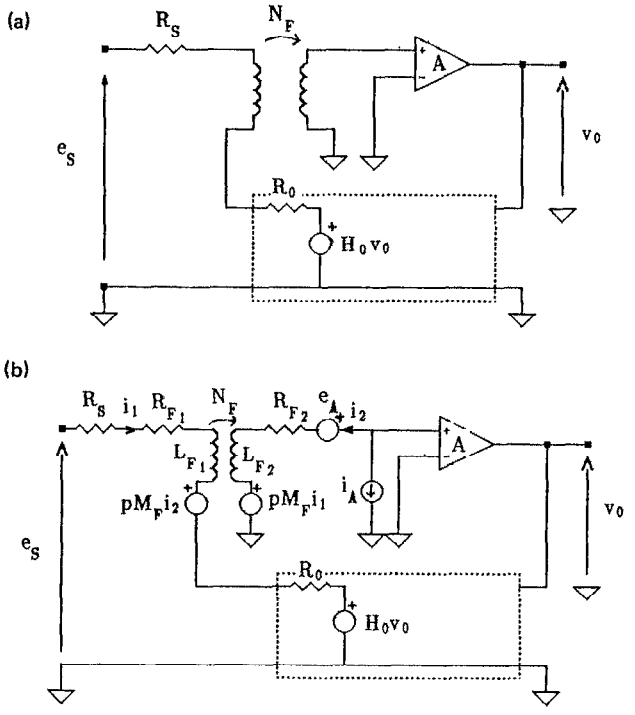

FIG. 1. (a) Sketch of the input transformer coupled feedback preamplifier. (b) Detailed view of the preamplifier allowing calculations of the signal and noise characteristics; the generators e_A and i_A are fictitious sources.

$$e_{n_T}^2 = e_{n_S}^2 + e_{n_{F_1}}^2 + e_{n0}^2 + (e_{n_A}^2 + e_{n_{F_2}}^2)\left|\frac{Z_1}{M_F\omega}\right|^2 + i_{n_A}^2\left|\frac{M_F^2\omega^2 + Z_1Z_2}{M_F\omega}\right|^2, \tag{3}$$

where all noise generators are considered to be uncorrelated, and where $e_{n_S}^2$, $e_{n_{F_1}}^2$, e_{n0}^2 [which act as e_S in expression (1)] are the thermal noise densities of R_S, R_{F_1}, and R_0, respectively, $e_{n_{F_2}}^2$, $e_{n_A}^2$ [which act as e_A in expression (1)] are the R_{F_2} and amplifier voltage noise contributions, and $i_{n_A}^2$ [which acts as i_A in expression (1)] is the input equivalent amplifier current noise density.

The input equivalent voltage and current noise densities of the preamplifier can easily be deduced from the $R_S = 0$ and $R_S = \infty$ limits of expression (3) and expressed as

$$e_n^2 = e_{n_{F_1}}^2 + e_{n0}^2 + \left[1 + \left(\frac{R_{F_1} + R_0}{L_{F_1}\omega}\right)^2\right]\left(\frac{e_{n_A}^2 + e_{n_F}^2}{N_F^2}\right) + \left[\left(R_0 + R_{F_1} + \frac{R_{F_2}}{N_F^2}\right)^2 + \left(\frac{(R_{F_1} + R_0)R_{F_2}}{N_F^2 L_{F_1}\omega}\right)^2\right]N_F^2 i_{n_A}^2, \tag{4}$$

$$i_n^2 = \frac{(e_{n_A}^2 + e_{n_{F_2}}^2)}{N_F^2 L_{F_1}^2\omega^2} + \left[1 + \left(\frac{R_{F_2}}{N_F^2 L_{F_1}\omega}\right)^2\right]N_F^2 i_{n_A}^2. \tag{5}$$

Since (4) and (5) are both functions of e_{n_A}, $e_{n_{F_2}}$, and i_{n_A}, some degree of correlation relates them, but this only matters close to the optimal source impedance and can thus be discarded for simplicity in the further discussion.

In the high-frequency limit, (4) and (5) become

$$e_n^2 \simeq e_{n_{F_1}}^2 + e_{n0}^2 + \frac{e_{n_A}^2 + e_{n_{F_2}}^2}{N_F^2} + \left(R_0 + R_{F_1} + \frac{R_{F_2}}{N_F^2}\right)^2 N_F^2 i_{n_A}^2, \tag{6}$$

$$i_n^2 \simeq N_F^2 i_{n_A}^2. \tag{7}$$

Compared to the ideal situation which leads as expected to an unmodified amplifier noise energy ($e_n i_n = e_{n_A} i_{n_A}$) and an optimal source resistance divided by N_F^2, some additive terms which come in (6) from the input transformer losses and from the feedback equivalent resistance R_0 have to be minimized. Such an objective requires a careful design of the input transformer. The magnetic losses can be made negligible by a proper choice of the core pot and ohmic losses minimized, for a given wiring section S, resistivity ρ, and mean turn length l when both winding sections are equal. In these conditions, the equivalent ohmic resistance of the transformer referred to the input expresses as

$$R_{TF} \simeq 4(\rho l/KS)N_{F_1}^2, \tag{8}$$

where K stands for the winding filling factor and N_{F_1} for the number of turns of the primary coil.

Moreover, Eq. (2) shows (all others conditions taken constant) that the input self-impedance of the transformer, which varies as $N_{F_1}^2$ and as the specific inductance of the core pot, must be chosen as high as possible in order to lower the low cutoff frequency f_0. Such a condition goes conversely with the R_{TF} minimization and leads to a compromise. We have chosen to set the transformer input noise contribution,

$$e_{n_{F_1}}^2 + (e_{n_{F_2}}^2/N_F^2),$$

at the same level as that of the amplifier one ($e_{n_A}^2/N_F^2$), the other terms in (6) being in practice of negligible effect. From (2) and (8) we obtain, therefore, within these conditions,

$$N_F^2 \simeq \frac{\pi e_{n_A}^2 KSA_l f_0(1 + AH_0N_F)}{8k_BT\rho l(R_S + R_0 + R_{F_1})}, \tag{9}$$

where A_l is the specific inductance of the core pot. Equation (9) relates the optimal N_F value to the desired amplifier parameters, operating conditions, and technological constraints. A quick numerical evaluation of (9) shows

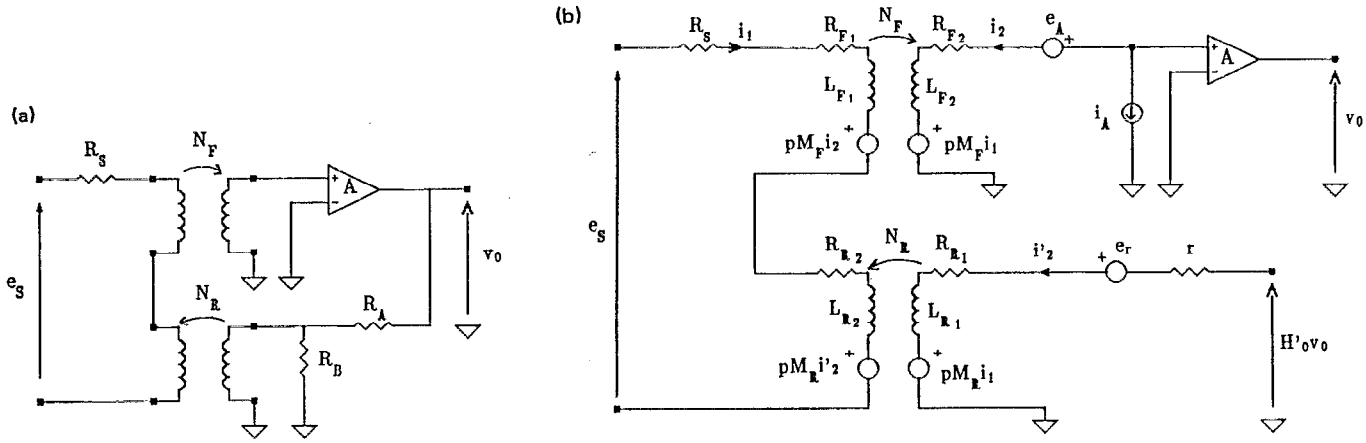

FIG. 2. (a) Sketch of an input and feedback transformer coupled preamplifier. (b) Detailed view of the input and feedback transformer coupled structure; the generators e_A, i_A, and e_r are fictitious sources allowing calculations of the system noise density.

that N_F ranges from 20 to 60 and shows that $e_n \simeq 60$ pV/$\sqrt{\text{Hz}}$ can be achieved.

III. THE LOW-NOISE INPUT AND FEEDBACK TRANSFORMER COUPLED DIFFERENTIAL STRUCTURE

Consider now the preamplifier structure shown in Fig. 2(a). It differs from that of Fig. 1 by the addition of a transformer T_R in the feedback loop, which first allows us to operate in a differential mode (a major feature for the detection of low-level signals) and, since $N_R \ll 1$, to easily put the R_0 resistance of the feedback path (Fig. 1) in the mΩ range. This feedback transformer T_R also behaves as a high-pass device, which brings some modifications of the low-frequency transfer and noise characteristics, which we briefly review now.

A. Signal analysis

From Fig. 2(b), the input–output transfer function can be obtained easily and expressed as

$$\frac{V_0}{e_s} = G_0 p^2 \frac{1 + [(r + R_{R_1})/L_{R_1} p]}{p^2 + \alpha\omega_0 p + \omega_0^2}, \tag{10}$$

where p is the Laplace complex variable and with

$$G_0 = \frac{AN_F}{1 + H'_0 AN_F N_R}, \quad H'_0 = \frac{R_B}{R_A + R_B}, \tag{11}$$

$$\omega_0^2 = \frac{(R_S + R_{F_1} + R_{R_2})(r + R_{R_1})}{L_{R_1} L_{F_1}(1 + H'_0 AN_F N_R)}, \quad r = \frac{R_A R_B}{R_A + R_B}, \tag{12}$$

and

$$\alpha = \frac{1}{\sqrt{(R_S + R_{F_1} + R_{R_2})(r + R_{R_1})}} \times \frac{L_{R_1}(R_S + R_{F_1} + R_{R_2}) + (L_{F_1} + L_{R_2})(r + R_{R_1})}{\sqrt{L_{F_1} L_{R_1}(1 + H'_0 AN_F N_R)}}. \tag{13}$$

Equation (10) shows that the preamplifier transfer function is the sum of a bandpass and of a high-pass second-order-type parts. In the practical design, the bandpass term is of low effect since $L_{R_1}\omega/(r + R_{R_1}) > 2$ in the frequency range of interest; furthermore, a peaked response is expected for a low source resistance up to the critical value defined by the $\alpha = \sqrt{2}$ condition in (13).

B. Noise analysis

In a similar way as in Sec. II B, the effect of the circuit noise sources can be referred back to the preamplifier input. Since the system transfer function is of second-order type, complete expressions are rather complex; therefore, only their asymptotic forms are given in Table I, leaving out a limited frequency range lying in close proximity to ω_0.

Thus, from Table I, the high-frequency input equivalent noise characteristics are expressed as

TABLE I. Input equivalent voltage and current noise densities of the various generators involved in the circuit. For simplicity, only the asymptotic expressions in the low- and high-frequency limits are given.

α_i		$e_n(\alpha_i)$	$i_n(\alpha_i)$
$e_{n_{F_1}}$, $e_{n_{R_2}}$, e_{n_A}	$\omega \to 0$	α_i	0
		$\frac{(R_{F_1} + R_{R_2})}{L_{F_1}\omega} \frac{\alpha_i}{N_F}$	$\frac{1}{L_{F_1}\omega} \frac{\alpha_i}{N_F}$
$e_{n_{F_2}}$	$\omega \to \infty$	α_i / N_F	0
i_{n_A}	$\omega \to 0$	$\frac{R_{F_2}}{N_F^2} \frac{(R_{F_1} + R_{R_2})}{L_{F_1}\omega} N_F \alpha_i$	$\frac{R_{F_2}}{N_F^2 L_{F_1}\omega} N_F \alpha_i$
	$\omega \to \infty$	$[R_{F_1} + R_{R_2} + N_R^2(R_{R_1} + r)] N_F \alpha_i$	$N_F \alpha_i$
$e_{n_{R_1}}$	$\omega \to 0$	0	0
e_{nr}	$\omega \to \infty$	$N_R \alpha_i$	0

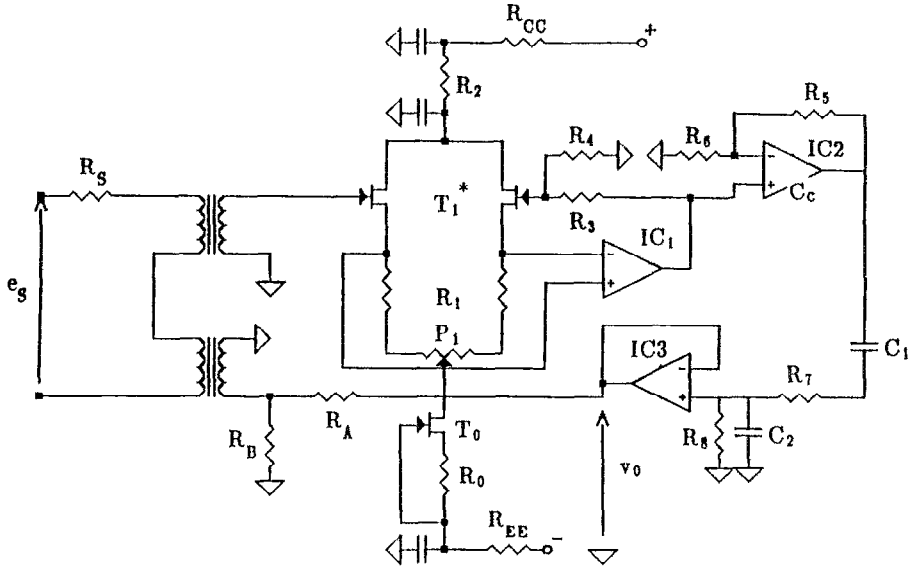

FIG. 3. Full schematics of the preamplifier. *Transistors*: T_1^*: 2×2 2SK170; T_0: 2N6550. *Integrated circuits*: IC_1: LT1028; IC2: AD844; IC3: AD845. *Transformers*: Siemens 41×25 pot cores, N48 ferrite material. *Resistances*: R_0: 100 Ω; R_1: 511 Ω; R_2: 237 Ω; R_3: 383 Ω; R_4: 10 Ω; R_5: 511 Ω; R_6: 38.3 Ω; R_7: 6.19 kΩ; R_8: 1 MΩ; R_{CC}: 43 Ω; R_{EE}: 43 Ω; P_1: 47 Ω. *Capacitors*: C_1: 1 μF; C_2: 5.6 μF; C_c: 2.2 nF; all unspecified capacitors are 220 + 0.1 μF.

$$e_n^2|_{\omega\to\infty} = e_{n_{F_1}}^2 + \frac{e_{n_{F_2}}^2}{N_F^2} + e_{n_{R_2}}^2 + N_R^2 e_{n_{R_1}}^2 + N_R^2 e_{nr}^2 + \frac{e_{n_A}^2}{N_F^2} + [R_{F_1} + R_{R_2} + N_R^2(R_{R_1} + r)]^2 N_F^2 i_{n_A}^2 \quad (14)$$

and

$$i_n^2|_{\omega\to\infty} = N_F^2 i_{n_A}^2, \quad (15)$$

while in the low-frequency limit it becomes

$$e_n^2|_{\omega\to 0} = e_{n_{F_1}}^2 + e_{n_{R_2}}^2 + \left(\frac{R_{F_1} + R_{R_2}}{L_{F_1}\omega}\right)^2 \left(\frac{e_{n_A}^2 + e_{n_{F_2}}^2}{N_F^2}\right) + \left(\frac{R_{F_2}}{N_F^2}\frac{(R_{F_1} + R_{R_2})}{L_{F_1}\omega}\right)^2 N_F^2 i_{n_A}^2 \quad (16)$$

and

$$i_n^2|_{\omega\to 0} = \frac{e_{n_A}^2 + R_{F_2}^2 i_{n_A}^2}{(L_{F_1}\omega N_F)^2}. \quad (17)$$

Equation (14) shows that in order to obtain the best results in the high-frequency limit, the feedback transformer has to offer an input equivalent resistance as weak as possible; its characteristics must then lie in the same range as that of the input transformer, which leads to a $N_R N_F$ product close to unity. Furthermore, since the resistive feedback path brings a $N_R^2 e_{nr}^2$ term, its equivalent resistance must also be taken low.

Finally, Eq. (16) indicates that several terms increase from their high-frequency limit as $[(R_{F_1} + R_{R_2})/L_{F_1}\omega]^2$; from Eq. (2) it is clear that this crossover point corresponds to the $R_S = 0$ open-loop low cutoff frequency of the preamplifier which has to be minimized.

IV. PREAMPLIFIER DESCRIPTION AND CHARACTERISTICS

We shall now turn to the full description of the preamplifier schematics shown in Fig. 3. Besides the requirements resulting from the above analysis, the design has also taken into account the high-frequency limitations coming mainly from the input transformer self-resonance.

Let us first consider the technological specifications of the input and feedback transformers. They are based on the Siemens 41×25 pot cores made of low-loss N 48 ferrite material.[6] The total air gap of the pot cores was initially 0.18 mm and the corresponding specific inductance 1250 nH. Since the magnetic losses of the transformers were negligible compared to the ohmic ones, the pot has been machined in order to increase the specific inductance up to 6000 nH. The primary and secondary coils are wound on individual coil formers. L_{F_1} and L_{R_2} inductances are made of one-layer joint turns while L_{F_2} and L_{R_1} are coiled irregularly on seven-section coil formers, which reduces their parasitic capacitance. The two transformers are placed inside soft iron cylindrical boxes which act as shields against external magnetic disturbances. The transformers' main mechanical and electrical characteristics are listed in Table II.

The active part of the circuit can be split into three blocks: a differential input low-noise amplifier (T_1^*,IC_1), an intermediate stage (IC_2), and an output buffer which

TABLE II. Mechanical and electrical characteristics of the input and feedback transformers.

	T_F transformer	T_R transformer
Transformation ratio	$N_F = 30$	$N_R = 1/20$
Primary coil	10 turns Cu wire, Φ 1 mm $R_{F_1} = 34\,\text{m}\Omega, L_{F_1} = 575\,\mu\text{H}$	160 turns Cu wire, Φ 0.25 mm $R_{R_1} = 3.8\,\Omega, L_{R_1} = 180\,\text{mH}$
Secondary coil	300 turns Cu wire, Φ 0.12 mm $R_{F_2} = 47\,\Omega, L_{F_2} = 515\,\text{mH}$	8 turns Cu wire, Φ 1.6 mm $R_{R_2} = 8\,\text{m}\Omega, L_{R_2} = 465\,\mu\text{H}$

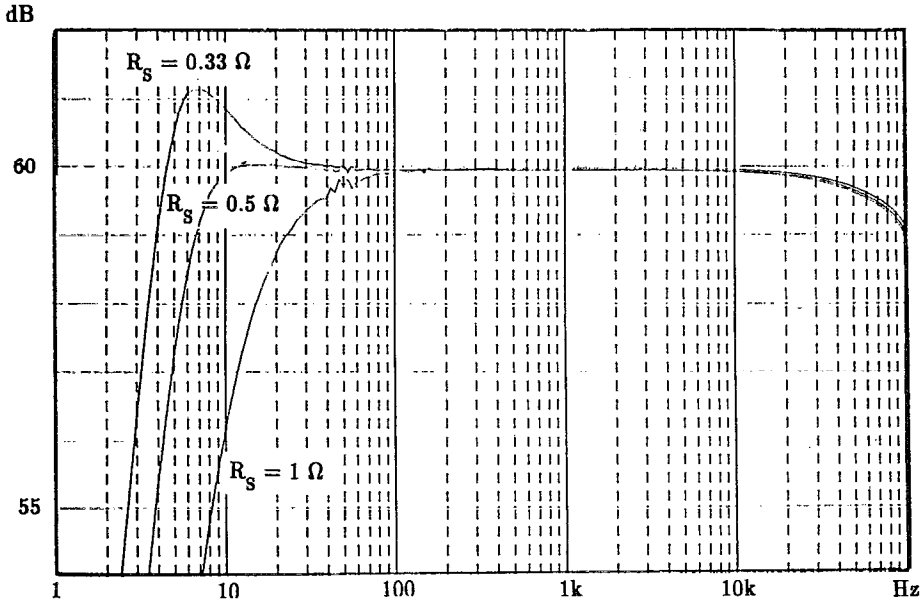

FIG. 4. Preamplifier transfer frequency response as a function of the source resistance; $R_S = 0.5\ \Omega$ is the critical value.

feeds the resistive low-impedance feedback path. The field-effect transistor (FET) differential common drain pair (T_1^*) uses a parallel association of 2SK170 Toshiba transistors[7] (two FETs on each side), which both reduces the input voltage and current equivalent noise densities and provides a low-input capacitance ($\simeq$20 pF). This stage feeds a low-voltage noise LT 1028 operational amplifier[8] whose overall gain is fixed to about 40 by the R_3/R_4 resistance ratio; a -6 dB per octave rolloff is obtained by the use of the capacitor C_c. This second stage is ac coupled to the unity gain buffer in order to roughly null the dc current in the return path. Finally, the R_7,R_8,C_2 lag circuit ensures the overall preamplifier stability at high frequency. The open-loop and input–output gains are 17 and 10^3, respectively, in the high-frequency range. Furthermore, the amplifier noise density e_{n_A} settles to about 1.4 nV/$\sqrt{\text{Hz}}$ at frequencies higher than 150 Hz (crossover point), while i_{n_A}—which increases with frequency—is close to 50 fA/$\sqrt{\text{Hz}}$ at 100 kHz.

The transformer and amplifier characteristics have been adjusted in order to operate between 10 Hz and 100 kHz. Figure 4 shows the preamplifier frequency response as a function of the source resistance R_S. For the critical one, the -1 dB bandwidth extends from 7 Hz to 100 kHz. The common mode gain was also measured; up to 15 kHz, it increases at a 20 dB per decade rate and settles to -103 dB at the line frequency. Beyond 15 kHz, the common mode gain increases at a rate of 40 dB per decade.

The preamplifier experimental noise density is plotted in Fig. 5 for a $R_S = 0.5\ \Omega$ source resistance. At high frequency, the noise level lies close to 100 pV/$\sqrt{\text{Hz}}$ when R_S is placed at 300 K and it lowers to 80 pV/$\sqrt{\text{Hz}}$ if R_S is cooled down to 77 K. From these measurements, it be-

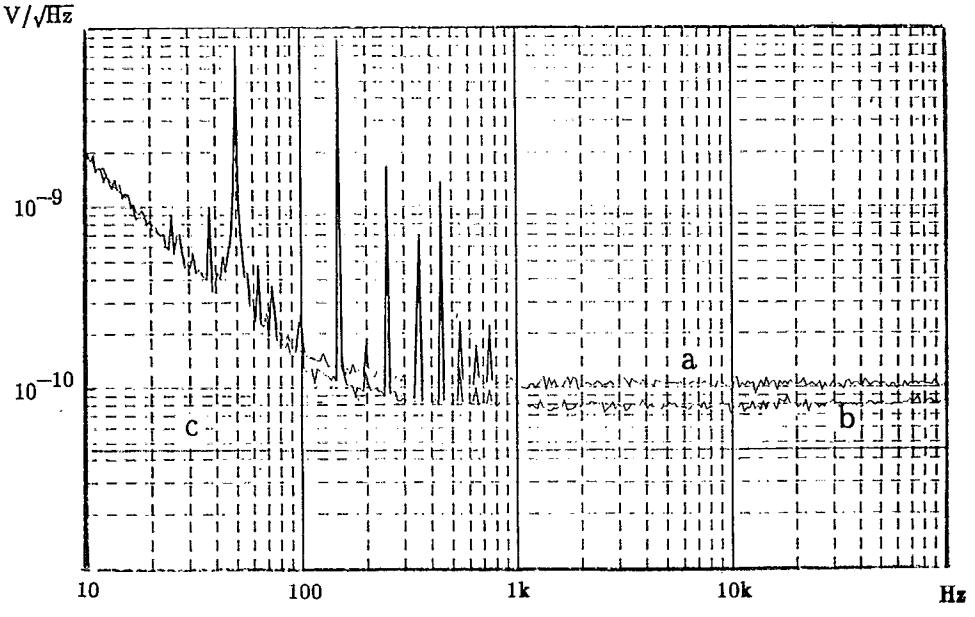

FIG. 5. Preamplifier input equivalent noise density from 10 Hz to 100 kHz for a $R_S = 0.5\ \Omega$ source resistance at 300 K [curve (a)] or at 77 K [curve (b)]. The (c) horizontal line marks the 77-K noise level of a 0.5-Ω resistance.

comes $e_n|_{\omega\to\infty} \simeq 65\ \mathrm{pV}/\sqrt{\mathrm{Hz}}$, in quite good agreement with the calculations from (14). In the high-frequency limit, the current noise i_n goes as i_{n_A} in (15) and increases with frequency; it settles to about 1.5 $\mathrm{pA}/\sqrt{\mathrm{Hz}}$ at 100 kHz. This leads to an overall energy resolution about $\sqrt{2}$ higher than that expected in an ideal case. Elsewhere, as discussed in Sec. III, e_n increases as ω^{-1} at low frequency ($f \leqslant 120$ Hz), which shows that the preamplifier open-loop low cutoff frequency must also be taken into account in the design.

[1] G. V. Pallotino and T. Lupi, Rev. Sci. Instrum. **61**, 2436 (1990).
[2] R. B. Hallgren, Rev. Sci. Instrum. **59**, 2070 (1988).
[3] C. D. Motchenbacher and F. C. Fitchen, *Low Noise Electronic Design* (Wiley, New York, 1973).
[4] Y. Netzer, Proc. IEEE **69**, 728 (1981).
[5] D. Bloyet, J. Lepaisant, and E. Varoquaux, Rev. Sci. Instrum. **56**, 1763 (1985).
[6] "Siemens Ferrites Data Book," 1986/87.
[7] "Small Signal Transistor Semiconductor Data Book," Toshiba Corp.
[8] Linear Technology Corporation, 1630 McCarthy Blvd., Milpitas, CA 95035-7487.